Science of the Total Environment 1004 (2025) 180789

Contents lists available at ScienceDirect

Science of the Total Environment

journal homepage: www.elsevier.com/locate/scitotenv

Action mechanism as a cause of chronic constipation of inhaled and intravenously injected polystyrene nanoplastics in ICR mice

Su Jeong Lim [a,1], Yun Ju Choi [a,1], Ji Eun Kim [a], Hee Jin Song [a], Ayun Seol [a], Su Ha Wang [a], Ji Eun Sung [a], Ye Eun Ryu [a], Ye Ryeong Kim [a], Woo Bin Yun [b], Miran Jang [c], Sungbaek Seo [a], Dae Youn Hwang [a,*]

[a] Department of Biomaterials Science (BK21 FOUR Program)/Life and Industry Convergence Research Institute/Laboratory Animal Resources Center, College of Natural Resources & Life Science, Pusan National University, Miryang 50463, Republic of Korea
[b] Department of Biology, University of Toronto Mississauga, ON L5L 1C6, Canada
[c] Department of Food Technology and Nutrition, Inje University, Gimhae 50834, Republic of Korea

HIGHLIGHTS

- Successful detection of inhaled nanoplastics (NPs) in lung, liver, kidney and intestine
- Observation of chronic constipation phenotypes in NPs-inhaled ICR mice for 2 weeks
- Verification of same phenotypes in ICR mice intravenously injected with NPs
- Novel scientific evidences of NPs as a possible cause for chronic constipation

GRAPHICAL ABSTRACT

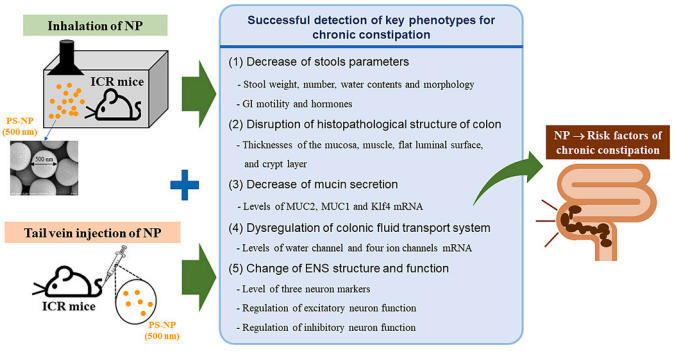

ARTICLE INFO

Keywords:
Plastics
Colon
Defecation
Mucin
ENS

ABSTRACT

The inhalation effects of airborne nanoplastics (NPs) on the gastrointestinal (GI) tract are rarely investigated, with most studies focusing only on the lungs and other organs. This study examined the changes in the key constipation phenotypes, mucin secretion, water and ion balance, and enteric nervous system (ENS) function in ICR mice after inhalation of polystyrene (PS)-NPs with 500 nm size for two weeks to determine if inhaled NPs can cause constipation. Significant constipation phenotypes, including the weight, water contents and morphology of stools, GI motility, intestinal length, histopathological structure of the colon, and concentration of GI hormone, were detected in NPs-inhaled ICR mice compared to a Vehicle-treated group. In addition, NPs-induced defecation delay was accompanied by a decrease in mucin secretion, suppressed transcription of mucin-related genes, and abnormal regulation of the colonic fluid transport system, including water and ions. NPs-inhaled mice showed a decrease in the neuronal cell density and dysfunction of excitatory neurons and inhibitory neurons in the ENS of the colon. Moreover, similar phenotypes for constipation were verified in ICR mice injected intravenously with

* Corresponding author at: Department of Biomaterials Science (BK21 FOUR Program), College of Natural Resources & Life Science, Pusan National University, 1268-50 Samrangjin-ro Samrangjin-eup Miryang-si, Gyeongsangnam-do 50463, Republic of Korea.
E-mail address: dyhwang@pusan.ac.kr (D.Y. Hwang).
[1] This author equally contributed to this study.

https://doi.org/10.1016/j.scitotenv.2025.180789
Received 6 August 2025; Received in revised form 21 October 2025; Accepted 21 October 2025
Available online 31 October 2025

NPs. Therefore, these results provide the first scientific evidence that inhalation and intravenous injection of PS-NPs can be considered as one of novel causes of constipation.

1. Introduction

Nanoplastics (NPs) derived from plastic bags, bottles, personal care products, construction materials, and clothing are exposed to humans through three major routes, including ingestion, inhalation, and dermal penetration (Sun and Wang, 2023). Among them, inhalation is an important route for depositing NPs or microplastics (MPs) in the respiratory system, including the lungs and blood vessels (Saha and Saha, 2024). Most inhaled NPs (~87 %) with various types accumulate in the lungs as their final destination and cause damage or functional injuries (Pauly et al., 1998). The inhalation of polystyrene (PS)-NPs induces pulmonary fibrosis, oxidative stress, inflammatory response, apoptosis, collagen deposition, mitochondrial dysfunction, autophagy stimulation, and ferroptosis activation in the lung tissues of animals (Li et al., 2022a; Wu et al., 2024; Yang et al., 2023). In addition, similar injuries or responses in lung tissues have been detected after inhaling polypropylene (PP) and polyvinyl chloride (PVC) NPs (Danso et al., 2022). The inhalation of tire wear NPs (TWNPs) induces ventilation dysfunction, fibrotic pathological changes, and epigenetic biomarkers attenuation (Li et al., 2022b). The inflammatory infiltrations and activation of the NLRPS/Cas-1/IL-1β signaling pathway were detected after the intratracheal administration of amine PS-NPs (APS-NPs) (Wu et al., 2023). On the other hand, a few studies have examined the effects of inhaled NPs on other organs besides the lung. The inhaled PS-NPs with 40 nm size induced remarkable hepatotoxicity accompanied by increasing concentrations of alanine transaminase (ALT), aspartate aminotransferase (AST) and alkaline phosphatase (ALP), decreasing cholinesterase (CHE), histological abnormality, inflammation enhancement, and fibrosis in the liver tissue (Ge et al., 2024). Significant cardiotoxicity, such as increased cardiac injury markers, imbalance between oxidase and antioxidase activity, structural and ultrastructural damage, and inflammatory responses, were detected after respiratory exposure to PS-NPs (Zhang et al., 2023). Nevertheless, no studies have been conducted on the effects of NPs inhalation or the gastrointestinal (GI) response to NPs, despite several studies on oral administration.

Several types of NPs administered orally to experimental animals induced damage or injuries to colon tissues. Most are the histopathological, cytological, and ultrastructural changes in colon tissue after treatment with PS, polyethylene (PE), poly (ethylene terephthalate) (PET), PVC, PP, oxidized PE (Ox-PE), and benzo[*a*]pyrene (B(*a*)P)-loaded aged PS (Choi et al., 2021; Xie et al., 2022; Wang et al., 2023; Shaoyong et al., 2023). In addition, the compositional changes in the colon microflora and inflammation were widely detected in PE, PS, PET, PP, PVC, and Ox-PE, B(*a*)P)-loaded aged PS materials-based NPs treated animals (Li et al., 2020; Xie et al., 2022; Wang et al., 2023; Shaoyong et al., 2023). Some other injuries, including GI motility, GI hormones, mucin secretion, permeability, immune cell composition, oxidative stress, and autophagy, were induced in the colon after treatment with various types of NPs (Choi et al., 2021; Sun et al., 2021; Wang et al., 2023; Shaoyong et al., 2023). Furthermore, oral administration of PS-NPs induced significant constipation-related phenotypes, while additional symptoms, including decreased mucin secretion, shortened colon length, and downregulation of tight junction, were observed in animals treated with other materials-based NPs, such as PE, and B(*a*)P-loaded aged PS (Choi et al., 2021; Sun et al., 2021; Wang et al., 2023; Shaoyong et al., 2023). Nevertheless, no studies have examined whether other exposure routes of NPs can cause constipation.

This study tested the hypothesis that inhaled NPs can cause constipation through the abnormal regulation of stool formation and defecation. Therefore, various phenotypes and action mechanisms of constipation were analyzed in ICR mice after inhalation and intravenous injection of 500 nm PS-NPs.

2. Materials

2.1. Characterization of nanoplastic

An aqueous suspension (25 mg/mL) of NPs, with a mean particle size of 500 nm and a density range of 1.04–1.06 g/cm^3, was obtained from Sigma–Aldrich Co. (St. Louis, MO, USA). Their morphological characterization was conducted using scanning electron microscopy/energy dispersive X-ray spectroscopy (SEM/EDX) (JEOL Ltd., Tokyo, Japan), with particle sizing verified using a Zetasizer Nano ZS90 (Malvern Instruments Inc., Malvern, UK), as described elsewhere (Choi et al., 2021). All suspensions were dispersed by sonication and diluted with water before inhalation and intravenous injection.

2.2. Animal study design

The Pusan National University-Institutional Animal Care and Use Committee approved the animal protocol for examining the inhalation and intravenous injection effects of NPs (Approval Number: PNU-2025-0429). The male ICR mice were housed in a specific pathogen-free (SPF) facility, accredited by the Korea Food and Drug Administration (KFDA, Accredited Unit Number: 000231) and the Association for Assessment and Accreditation of Laboratory Animal Care (AAALAC) International (Accredited Unit Number: 001525). They were provided a standard diet (Samtako BioKorea Inc., Osan, Korea) and filtered tap water with *ad libitum*. They were bred under a strict light cycle (light on for 12 h and dark for 12 h), temperature (23 ± 2 °C), and relative humidity control (50 ± 10 %).

The inhalation experiment was conducted using seven-week-old ICR mice (n = 24), and they were briefly divided into a 1× PBS inhaled group (Vehicle, n = 6) and three NPs-inhaled groups: low (LoNP-inhaled group, n = 6), medium (MiNP-inhaled group, n = 6), and high (HiNP-inhaled group, n = 6) concentrations. The optimal dosage for NPs inhalation was determined based on previous studies that examined the tissue accumulation and inhalation toxicity of PS-MPs and NPs. This particles were inhaled daily in three different dosages (4, 8, or 16 μg/mL) in a total volume of 8 mL/day for 30 min at 0.25 mL/min, using a non-heating compressor nebulizer (NE-C28, MRON DALIAN Co. LTD, Dalian, China). The Vehicle-inhaled group was received the same volume of a 1× PBS solution. After two weeks of NPs inhalation, all mice in each group were bred in metabolic cages to collect stools, urine, food, and water samples, and then, GI transit was analyzed using a charcoal meal (Supplement Fig. S1A).

The tail vein injection (Ti) experiment was conducted by grouping the ICR mice (n = 10) into 1× PBS-injected group (TiVehicle-injected group, n = 5) and NPs-injected group (TiNP-injected group, n = 5). A suspension of NP at 16 μg/mL was injected into the tails of ICR mice at a volume of 200 μL per day for two consecutive days, while 1× PBS was injected in the same way (Supplement Fig. S1B). Finally, all ICR mice were euthanized by trained researchers using CO_2 gas with a minimum purity of 99.0 % based on the American Veterinary Medical Association (AVMA) Guidelines for the Euthanasia of Animals. Furthermore, the GI tracts were harvested from the subset group of ICR mice for GI transit analyses. The mid-colon was collected for histopathological and molecular analyses.

2.3. Measurement of feeding behavior and stool parameter analysis

The average daily food intake and water consumption were

calculated from these measurements as described elsewhere (Choi et al., 2021). Also, the mice from the subset group were housed individually in metabolic cages (Daejong Ltd., Seoul, Korea) for 12 h to collect stools and urine without contamination. After harvesting at 10:00 a.m., the total number and weight of the stools were measured twice. The stool water content was calculated using the formula (A-B)/A × 100, where A represents the fresh stool weight and B is the stool weight after drying for 24 h at 60 °C. In addition, stool morphology was examined under a stereoscopic microscope, and abnormally and normally shaped stools were counted twice.

2.4. Measurement of gastrointestinal hormones transit and the tract length

The GI transit ratio was determined using the method described by Choi et al. (2021). After administrating a charcoal meal suspension composed of 3 % activated charcoal in 0.5 % methylcellulose (Sigma-Aldrich Co.), the mice were euthanized using CO_2, and the GI tract was collected. The GI transit ratio was calculated as follows: Charcoal transit ratio (%) = [(total small intestine length - distance traveled by charcoal) / total small intestine length] × 100.

2.5. Distribution of the nanoplastic in organs of mice

The liver, kidney, lung and intestine derived from each mouse were homogenized using a Polytron® Homogenizer PT 3100 D (KINEMATICA, Luzern, Switzerland). The collected pellet was digested in a piranha solution (H_2SO_4: H_2O_2 = 7:3) at room temperature for 4 h. After further collection, the NP fluorescence was measured in the pellet using a fluorescence reader (Spectramax i5D, Molecular Devices, Sunnyvale, CA, USA).

The distribution of intravenously injected NPs was analyzed by preserving the mid- colons, liver, spleen and lung in 1× PBS until cryosectioning, followed by embedding them in a mold containing OCT compound. After storing the mid-colon tissues at −80 °C for more than 24 h, these samples were sectioned to a 10 μm thickness using a cryostat microtome (Leica Biosystems, CM1860). The fluorescent signals of NPs with red color were observed in the mid-colon section using fluorescent spectroscopy.

2.6. Histopathological examination

The mid-colons of the mice were fixed in 10 % formalin for 48 h, embedded in paraffin, and sectioned into 4 μm slices. The sections were deparaffinized in xylene, rehydrated, and stained with hematoxylin and eosin (H&E, Sigma–Aldrich Co.). The mucosal thickness, luminal surface thickness, and goblet cell number were analyzed by optical microscopy using the Leica Application Suite (Leica Microsystems Ltd., Heerbrugg, Switzerland). For mucin staining analysis, the mid-colon sections were also stained using an Alcian Blue stain kit (IHC WORLD, Woodstock, MD, USA) after fixation, paraffin embedding, and sectioning. The stained sections were examined by optical microscopy for the histology evaluation.

2.7. Immunofluorescence staining analysis

Immunofluorescence (IF) staining was performed to detect C-kit in the mid-colon as described elsewhere (Choi et al., 2021). The trimmed colon tissues were fixed in 10 % formalin, embedded in paraffin, and sectioned at 4 μm. After deparaffinization and rehydration, the tissue sections were treated with a blocking buffer containing 10 % goat serum (Vector Laboratories, Inc., Burlingame, CA, USA) in a 1× PBS solution and incubated with anti-C-kit antibodies (1:200, DAKO, Kyoto, Japan). These sections were incubated with goat fluorescein isothiocyanate (FITC)-labeled anti-rabbit IgG (1:200, Thermo Fisher Scientific Inc., Wilmington, MA, USA), followed by additional washing and mounting. Finally, the green fluorescence was visualized using an EVOS M5000 Imaging System (Thermo Fisher Scientific Inc.).

2.8. Western blot analysis

The total proteins from the mid-colons of the mice were extracted using a Pro-Prep Protein Extraction Solution (Intron Biotechnology Inc., Seongnam, Korea) according to the manufacturer's protocol. After separation of total proteins (30 μg) on 4–20 % SDS-PAGE, the membranes were incubated overnight at 4 °C with primary antibodies (Supplement Table S1). After washing, the membranes were incubated with horseradish peroxidase (HRP)-conjugated goat anti-rabbit IgG (1:1000, Zymed Laboratories, South San Francisco, CA, USA) for 2 h at room temperature. The blots were developed using a Chemiluminescence Reagent Plus kit (Pfizer Inc., Gladstone, NJ, USA), and the signals were captured using a FluorChem® FC2 Imaging System (Alpha Innotech Corporation, San Leandro, CA, USA), equipped with a 1.92 MP digital camera. The band densities of proteins on the membrane were semi-quantified using the AlphaView Program, version 3.2.2 (Cell Biosciences Inc., Santa Clara, CA, USA).

2.9. RT-qPCR

After isolation of total RNA from frozen mid-colon, the cDNA was synthesized with SuperScript II reverse transcriptase (Thermo Fisher Scientific Inc.) using 4 μg of RNA and oligo-dT primers under the recommended conditions. Quantitative Real-Time PCR (RT-qPCR) was conducted using 2 μL of cDNA, 2× Power SYBR Green (Toyobo Life Science, Osaka, Japan), and specific primers (Supplement Table S2) under the following cycling conditions: 40 cycles at 95 °C for 15 s and 60 °C for 60 s. The fluorescence intensity was recorded at each extension step, and the threshold cycle (Ct) values were determined. Gene expression was normalized to β-actin using the $2^{-\Delta\Delta Ct}$ method.

2.10. Measurement of gastrointestinal hormone level

The cholecystokinin (CCK) and gastrin concentrations in the mid-colon tissue were measured using ELISA kits (Cusabio Biotech Co., Ltd., China) according to the manufacturer's instructions. After preparation of the tissue homogenates, the specific antibodies for each hormone were added to separate wells, followed by 1 h incubation at 37 °C. After washing, a streptavidin protein conjugated covalently to HRP solution was added to each well and incubated for another hour at 37 °C. And then, TMP One-Step Substrate Reagent was added, and the samples were incubated for 30 min at 37 °C. The reaction was quenched by adding a stop solution, and the absorbance of each well was read at 450 nm using a VersaMax Plate Reader (Molecular Devices).

2.11. Measurement of 5-hydroxytryptamine level

The 5-hydroxytryptamine (5-HT) levels in the mid-colon were measured using ELISA kits (ImmuSmol, Pessac, France) according to the manufacturer's protocol. After collecting the homogenates of tissue, 5-HT anti-serum was added, followed by incubation at 2–8 °C for 15–20 h. After washing, an enzyme conjugate solution was applied to each well and incubated for 30 min at room temperature. The substrate reagent was then added, with subsequent incubation for 30 min. Finally, the reaction was stopped with stop solution, and the absorbance of the mixture was read at 450 nm using a VersaMax Plate Reader (Molecular Devices).

2.12. Measurement of the acetylcholine level

The acetylcholine (ACh) levels were measured using an Acetylcholine Assay Kit (Cell Biolabs Inc., San Diego, CA, USA) according to the manufacturer's instructions. After preparation of the tissue homogenate,

the samples or standards were combined with the ACh reaction mixture in a light-protected 96-well plate and incubated on an orbital rotator at room temperature for 45 min. The colorimetric changes of the wells were measured using a Vmax plate reader (Molecular Devices).

2.13. Measurement of nitric oxide concentration in mid-colon

The concentration of nitric oxide (NO) in the mid-colon tissue was determined using the Griess reagent which have the principle of the Griess reaction involves a diazotization reaction (Invitrogen Co., Ltd., Carlsbad, CA, USA). After collecting the tissue homogenates using freeze-thaw cycle, the samples (100 μL) were added to 96-well plates and mixed with 100 μL of modified Griess reagent (Invitrogen, Carlsbad, CA, USA). The absorbance of each well was measured at 548 nm using a Versa max plate reader (Molecular Devices). A standard curve with increasing sodium nitrite ($NaNO_2$) concentrations was generated in parallel and used for quantification.

2.14. Statistical analyses

Briefly, a normality test was assessed using a Shapiro–Wilk test in SPSS 27.0 (IBM Co., Armonk, NY, USA) to determine whether all data has been drawn from a normally distributed population. The statistical significance between Vehicle- and NPs-inhaled groups was determined using the one-way analysis of variance (ANOVA), while those between TiVehicle- and TiNP-injected group was determined using the unpaired two-sample *t*-test. Also, Tukey multiple comparison tests were also applied to support results of ANOVA. All values used in this study are represented as the means ± SD. Furthermore, *p*-values <0.05 were considered significant.

3. Results

3.1. Physicochemical properties and intestinal distribution of nanoplastic

The physicochemical properties of PS-NPs were analyzed by measuring the morphological features, actual size, and electric charge of NPs using SEM and a size analyzer. NPs had a circular shape with a regular size (Fig. 1A). The measured size distribution and zeta potential of NPs were 593.83 ± 7.53 d.nm and − 35.98 ± 0.26 mV, respectively (Fig. 1B). These results show the possibility that NPs can be easily uptaken into cells. In addition, the inhaled NPs were detected at high levels in the intestine, liver, kidney and lung of ICR mice when compared to the Vehicle-inhaled mice (Fig. 1C and Supplement Fig. S2A). Therefore, the above results suggest that the inhalation of NPs is a suitable condition for analyzing their effects on intestinal diseases.

3.2. Effects of nanoplastic inhalation on the basic parameters for constipation

This study first investigated whether the inhalation of NPs affects the basic parameters for constipation of ICR mice. Hence, the changes in food intake, urine volume, and stool parameters, GI motility, intestinal length and concentration of GI hormone were analyzed in ICR mice after inhalation with three doses of NPs for two weeks. Significant changes were observed in most constipation parameters, even though food intake, urine volume and colon length were remained constant. The weight, number and water contents of stools were 46.23 %–68.50 % lower in the NPs-inhaled group than in the Vehicle-inhaled group (Fig. 2A). In particular, the number of normal stools among the total stools decreased significantly after the inhalation of NPs, while the number of abnormal stools, including the small, short, and irregular types, was constant (Fig. 2B). Also, the transit ratio of the charcoal meal was lower only in the HiNP-inhaled group than in the Vehicle-inhaled group and other NPs-inhaled groups, while the intestine length was shorter in the MiNP and HiNP-inhaled groups (Fig. 2C). Especially, the migration of stools was stagnant in the mid- and distal-colon despite the lack of significance in the changes of their length (Fig. 2D). The concentrations of the CCK and gastrin hormone that influence colonic motility were decreased in a dose-dependent manner after the inhalation of NPs (Fig. 2E). These results suggest that NPs induced a defecation delay was accompanied by a decrease in the stool parameters, GI motility, intestine length and concentration of GI hormone as well as colonic stagnation of stools in ICR mice.

3.3. Changes in the histopathological and cytological structure of the mid-colon

To investigate whether the defecation delay in NPs-inhaled mice is accompanied by changes in the histological structure of the mid-colon, alterations in the histopathological structures of the H&E-stained tissue were analyzed in the mid-colon of NPs-inhaled ICR mice. The thicknesses of the mucosa, muscle, flat luminal surface, and crypt layer were significantly lower in the NPs-inhaled group than in the Vehicle-inhaled group. Most of them exhibited a dose-dependent decrease pattern, even though the highest level was detected in the HiNP-inhaled group (Fig. 3A and B). In addition, a similar decrease pattern was detected in the number of goblet cells per crypt of Lieberkühn (Fig. 3A and B). Therefore, NPs-induced defecation delay is associated with significant abnormalities on the histopathological structure in the mid-colon of ICR mice.

3.4. Effects of nanoplastic inhalation on the mucin secretion ability and fluid transport system of the mid-colon

We next examined whether the inhibition of mucin secretion and dysregulation of the fluid transport system could be considered as a cause of NPs-induced defecation delays. To achieve these, alterations on the expression levels for mucin, water transporter and five ion channels were measured in the mid-colon of the NPs inhaled groups. The dark blue density indicated that the mucin proteins as well as the mRNA levels of mucin 2 (MUC2), MUC1, and Krüppel-like factor 4 (Klf4) genes were significantly lower in the NP-inhaled groups than in the Vehicle-inhaled group except for the LoNP-inhaled group (Fig. 4A). The transcription levels of aquaporin 3 (AQP3) and 8 genes decreased in a dose-dependent manner after the inhalation of NPs, while the water intake remained constant between Vehicle- and NPs-inhaled group (Fig. 4B and C). In addition, the inhibitory effects of NPs in AQPs transcription levels were completely reflected in the mitogen-activated protein kinase/nuclear factor kappa B (MAPK/NF-κB) pathway because AQP3 regulates the liquid water metabolic abnormalities and intestine permeability alteration via the MAPK/NF-κB pathway (Fig. 4D) (Zhan et al., 2020). Furthermore, the expression levels of four ion channel genes, including cystic fibrosis transmembrane conductance regulator (CFTR), anoctamin-1 (ANO-1), solute carrier family 26 member 3 (SLC26A3), and solute carrier family 26 member 6 (SLC26A6) were significantly higher in the NPs-inhaled groups than in the Vehicle-inhaled group, while the reverse pattern was detected in the transcription level of voltage-gated chloride intracellular channel 2 (CIC-2) chloride channel after NPs inhalation (Fig. 4E). These results suggest that NPs-induced defecation delay may be associated with decrease of mucin secretion and transcriptional downregulation of mucin-related gene as well as dysregulation of the MAPK/NF-κB signaling pathway-related fluid transport system in the mid-colon of ICR mice.

3.5. Effects of nanoplastic inhalation on the structure and function of enteric nervous system in the mid-colon

To investigate whether the abnormal structure and dysfunction of the enteric nervous system (ENS) could be considered as a cause of the NPs-induced defecation delays, alterations on the distribution of neuronal cells, and the regulatory factors of excitatory and inhibitory

A

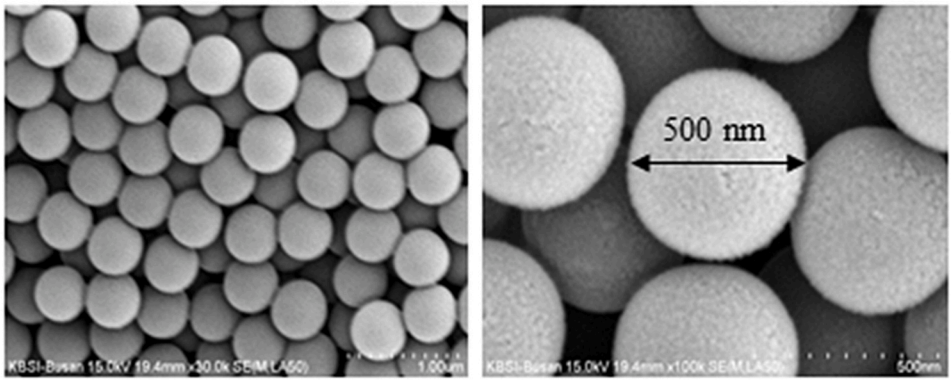

B

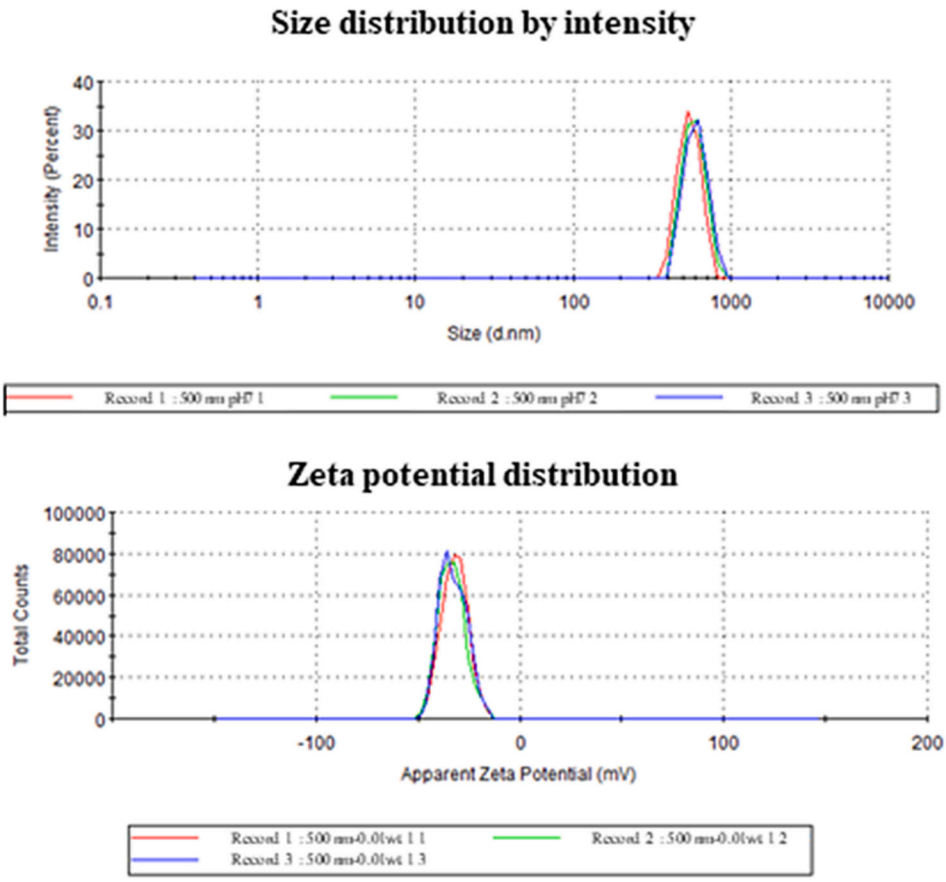

C

Categories	Vehicle	LoNP	MiNP	HiNP
Distribution of NP (μg/g)	0.01	8.77 ± 0.003	18.85 ± 0.002	37.47 ± 0.002

Fig. 1. Physicochemical properties and distribution of nanoplastics (NPs). (A) Scanning electron microscopy image of NPs at 10,000× and 20,000× magnification. (B) Size and zeta potential of NPs. (C) Accumulation of NPs in the intestine.

A

Categories	Vehicle	LoNP	MiNP	HiNP
Food intake (g/day)	5.14 ±0.45	4.59±0.44	4.21±1.13	4.35±0.50
Stool weight (g)	0.78 ±0.11	0.47±0.03*	0.41±0.05*	0.39±0.04*
Stool number (ea)	48.67±3.88	26.17±3.32*	24.50±4.42*	15.33±4.13*
Urine volume (mL)	1.40±0.19	1.40±0.24	1.53±0.16	1.58±0.29
Stool water contents (%)	68.78±4.40	56.26±3.44*	48.33±6.90*	42.63±5.78*

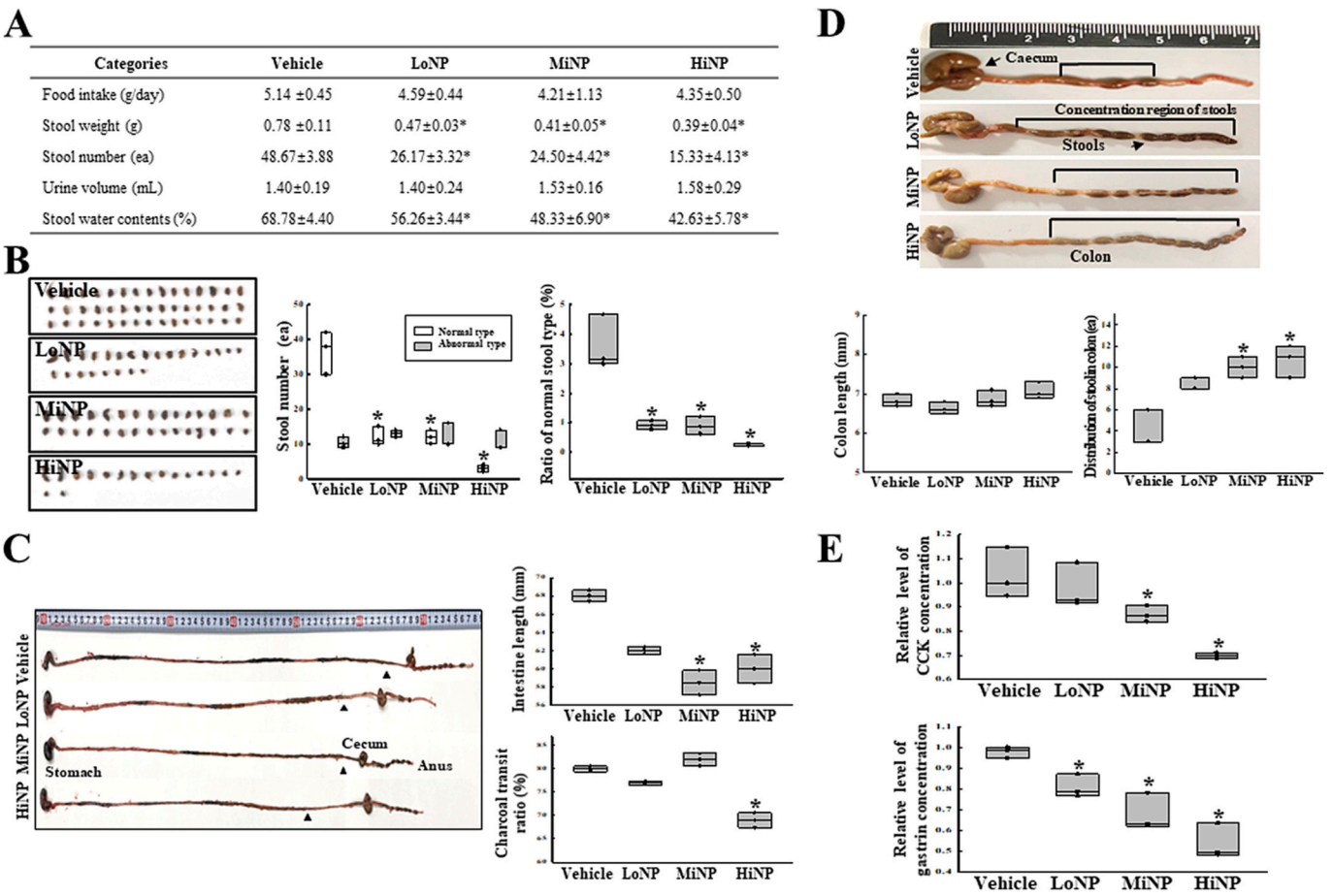

Fig. 2. Basic parameters for constipation of nanoplastics (NPs)-inhaled mice. (A) Food intake, urine volume, and stool parameters. (B) Morphological properties of stools. (C) Actual image showing the charcoal meal transit and intestine. (D) Morphology, length, and stool distribution of colon. (E) Concentrations of cholecystokinin and gastrin. The arrowhead indicates the position of the charcoal meal in the total gastrointestinal tract from the stomach to the anus. Three to five mice per group were used for sample collection, and each parameter was assayed in duplicate. The data are reported as the mean ± SD. *, $p < 0.05$ compared to the Vehicle-inhaled group.

neurons were analyzed in the mid-colon of the NPs-inhaled mice. The expression levels of the C-kit, protein gene product 9.5 (PGP9.5) and neuron-specific enolase (NSE) proteins for neurons were significantly decreased in a dose-dependent manner in all three NPs-inhaled groups, despite the highest reduction observed in the HiNP-inhaled group (Fig. 5A and B). Also, the 5-HT concentration and the expression of 5-HT receptors including 3AR, 3BR, 2AR, and 2BR were significantly decreased in the MiNP- and HiNP-inhaled group than in the Vehicle-inhaled group (Fig. 5C). The concentration of ACh was lower in the MiNP- and HiNP-inhaled group than in the Vehicle-inhaled group (Fig. 5D). These decreasing patterns were reversely reflected in the expression level of two types of muscarinic acetylcholine receptor (mAChR), including M2 and M3 (Fig. 5D). Furthermore, the changes in the mAChR downstream signaling pathway were accompanied by alterations in the ACh concentration and the level of mAChR expression (Fig. 5E). Moreover, the NO concentration and the expression level of inducible nitric oxide synthase (iNOS) were significantly increased in the NPs-inhaled group compared to the Vehicle-treated group, while an opposite decrease pattern was detected in the expression level of neuronal nitric oxide synthase (nNOS) in the NPs-inhaled group (Fig. 5F). Therefore, these results show that NPs-induced defecation delay may be tightly linked to the decrease in the density of neuronal cells, and the alternative regulation of excitatory and inhibitory neurons in the mid-colon of ICR mice.

3.6. *Verification of the role of nanoplastic as a cause of constipation through the intravenous injection of nanoplastic*

Finally, this study examined whether the systemic translocation of inhaled NPs to the colon through blood vessels can cause defecation delays. Therefore, changes in the stool parameters, histological structure, and mucin secretion were analyzed in the ICR mice after intravenous injections of NPs twice. The NPs injected via the tail vein were detected as fluorescence signals in frozen sections of colon tissue, while other tissue, including the liver, spleen, and lung, showed similar signals (Fig. 6A and Supplement Fig. S2B). The number, weight, water contents of stools and urine volume were significantly lower in the TiNP-injected group compared to the TiVehicle-injected group, even though their decrease rate was varied (Fig. 6B). In addition, a similar decrease pattern was observed in charcoal transit ratio and colon length. Most stools were delayed in the mid-colon of the TiNP-injected group, while stools were distributed evenly in the TiVehicle-injected group (Fig. 6C). Furthermore, NPs injected via the tail vein induced histopathological alterations in the mid-colon of mice. TiNP-injected group showed significant abnormality in the tube-like gland structure of the crypts, even though the muscle thickness and flat luminal surface thickness increased significantly in the same group (Fig. 6D). A similar decreasing pattern in colonic mucin secretion was observed in the TiNP-injected group (Fig. 6E). Therefore, the systemic translocation of NPs through blood vessels suggest that inhaled NPs may be associated with the action mechanism as cause of constipation.

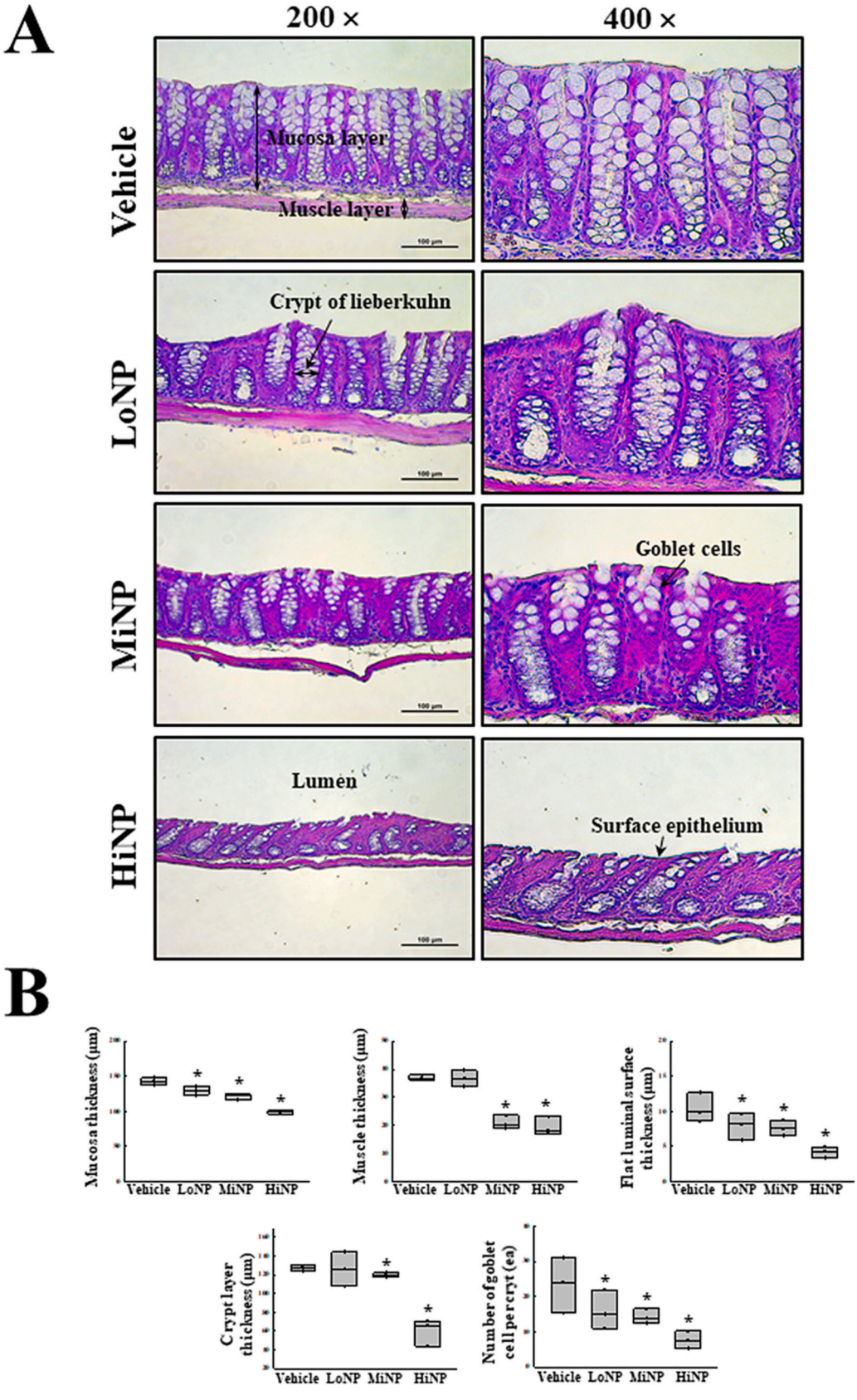

Fig. 3. Histopathological characteristics in the mid-colon of nanoplastics (NPs)-inhaled mice. (A) Histological structure of hematoxylin and eosin (H&E)-stained sections. The tissue sections of the mid-colons were stained using a H&E solution, and their structure was observed at 200× and 400× magnification using an optical microscope. (B) Histopathological parameters. These levels were determined using the Leica Application Suite. Three to five mice per group were used to prepare the H&E-stained sections, and the histopathological parameters for each slide were measured in duplicate. The data are reported as the mean ± SD. *, $p < 0.05$ compared to the Vehicle-inhaled group.

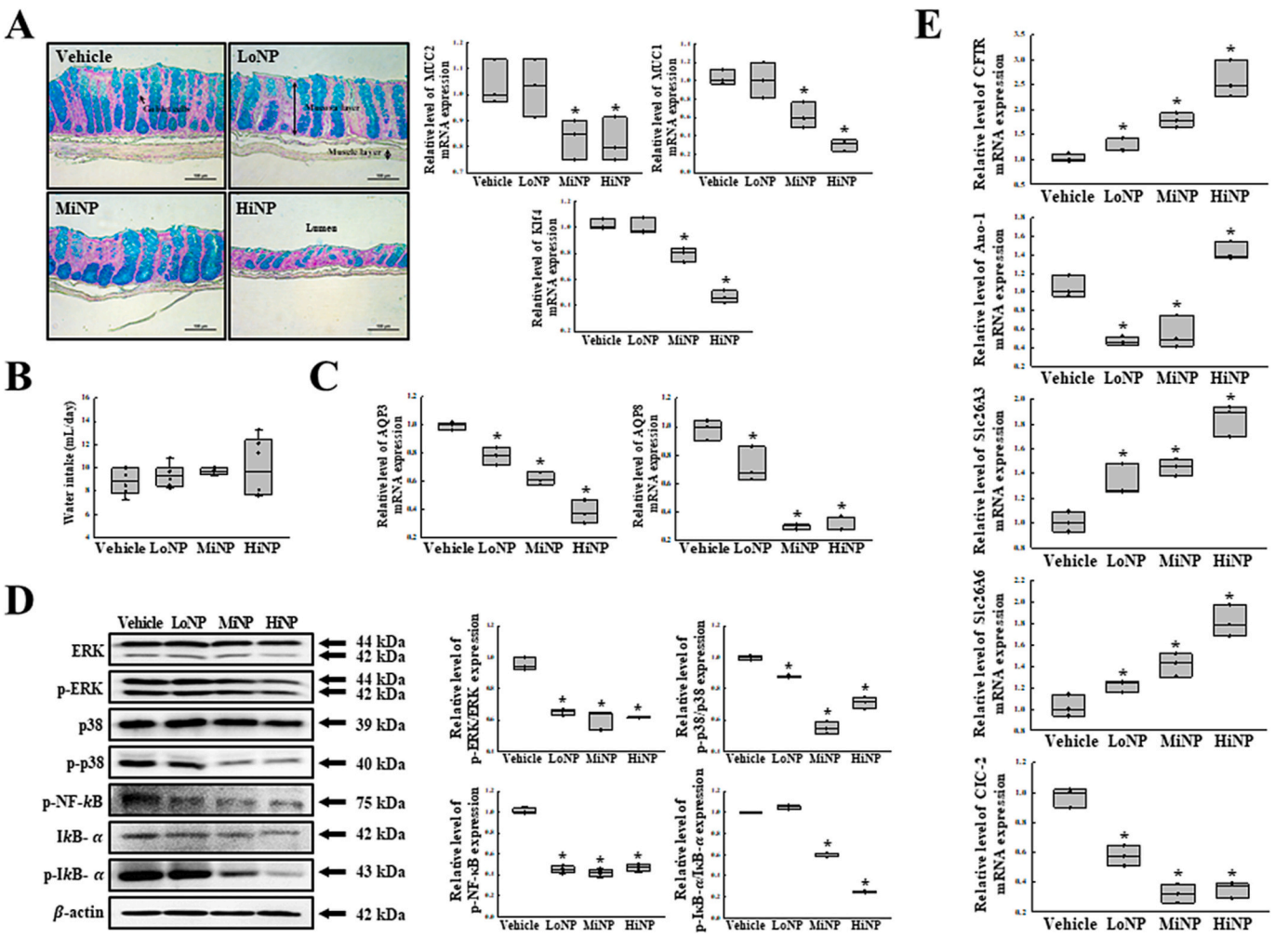

Fig. 4. Level of mucin secretion and parameters for fluid transport system in the mid-colon of nanoplastics (NPs)-inhaled mice. (A) Alcian blue-stained images for the mucin proteins and transcription levels of mucin-related genes. (B) Water intake. (C) Transcription levels of the aquaporin (AQP) 3 and 8 genes. (D) Expressions of the key mediators in the AQPs downstream signaling pathway. (E) Transcription levels of five ion channels including cystic fibrosis transmembrane conductance regulator (CFTR), anoctamin-1 (Ano-1), solute carrier family 26 member 3 (Slc26A3), solute carrier family 26 member 6 (Slc26A6) and chloride intracellular channel 2 (CIC-2). Three to five mice per group were used to prepare the stained sections, total RNA and tissue lysates, and each analysis were conducted in duplicate. The data are reported as the mean ± SD. *, $p < 0.05$ compared to the Vehicle-inhaled group.

4. Discussion

4.1. Effects of inhaled nanoplastic in colon-related diseases

The NPs inhaled from the atmospheric environment can primary deposit in the lung tissue through gravitational sedimentation and Brownian diffusion, which can lead to respiratory and lung diseases (Atis et al., 2005; Islam et al., 2023). After then, they transport and accumulate into other organs such as liver, spleen, brain, placenta, and kidneys. But, this transportation of NPs can be influenced by various physicochemical and biological factors including particle size, morphological properties, cellular uptake and biological barrier (Zhang et al., 2024). Therefore, more scientific evidences are required to clearly evaluate the impact of NPs in each organ. As part of these studies, the results of the present study provide the first scientific evidence that inhaled NPs with 500 nm size were transported to the colon through circulation system and can be caused chronic constipation in ICR mice. In particular, a study of the intravenous injection of NPs confirmed that the systemic translocation of NPs through the blood vessels may be closely linked to the induction of constipation. These results provide new evidence of the risk for inhaled NPs in humans, but further research is needed. Meanwhile, the previous studies have reported only the effects of inhaled NPs on cardiovascular damage. The accumulation of NPs in carotid artery plaques was increased the risk of heart attacks and strokes (Olatunji et al., 2024).

4.2. Co-relationship between constipation-related phenotypes and nanoplastic treatment

Only a few studies have provided indirect evidence for the co-relationship between constipation-related phenotypes and NPs treatment. First, the mucin secretion and relative abundances of gut microbiota, including *α-Proteobacteria* and *Firmicutes*, were significantly lower in the ICR mice continuously exposed to drinking water containing PS-NPs (0.5 and 50 μm size) for five weeks (Lu et al., 2018). In addition, the exposure of drinking water containing PS-MPs (5 μm) to pregnant ICR mice induced significant alterations in the composition of 14 bacteria species, mucin secretion, and transcription of the bacteria-related genes (Luo et al., 2019). The increase in bacterial abundance, number of gut microbial species, flora diversity, and inflammatory cytokine concentrations in serum was detected in the C57BL/6 mice treated with PS-MPs for five weeks (Li et al., 2020). Recently, strong direct evidence for this relationship was investigated in ICR mice administered PS-MPs orally (500 nm) for two weeks. They exhibited significant phenotypes

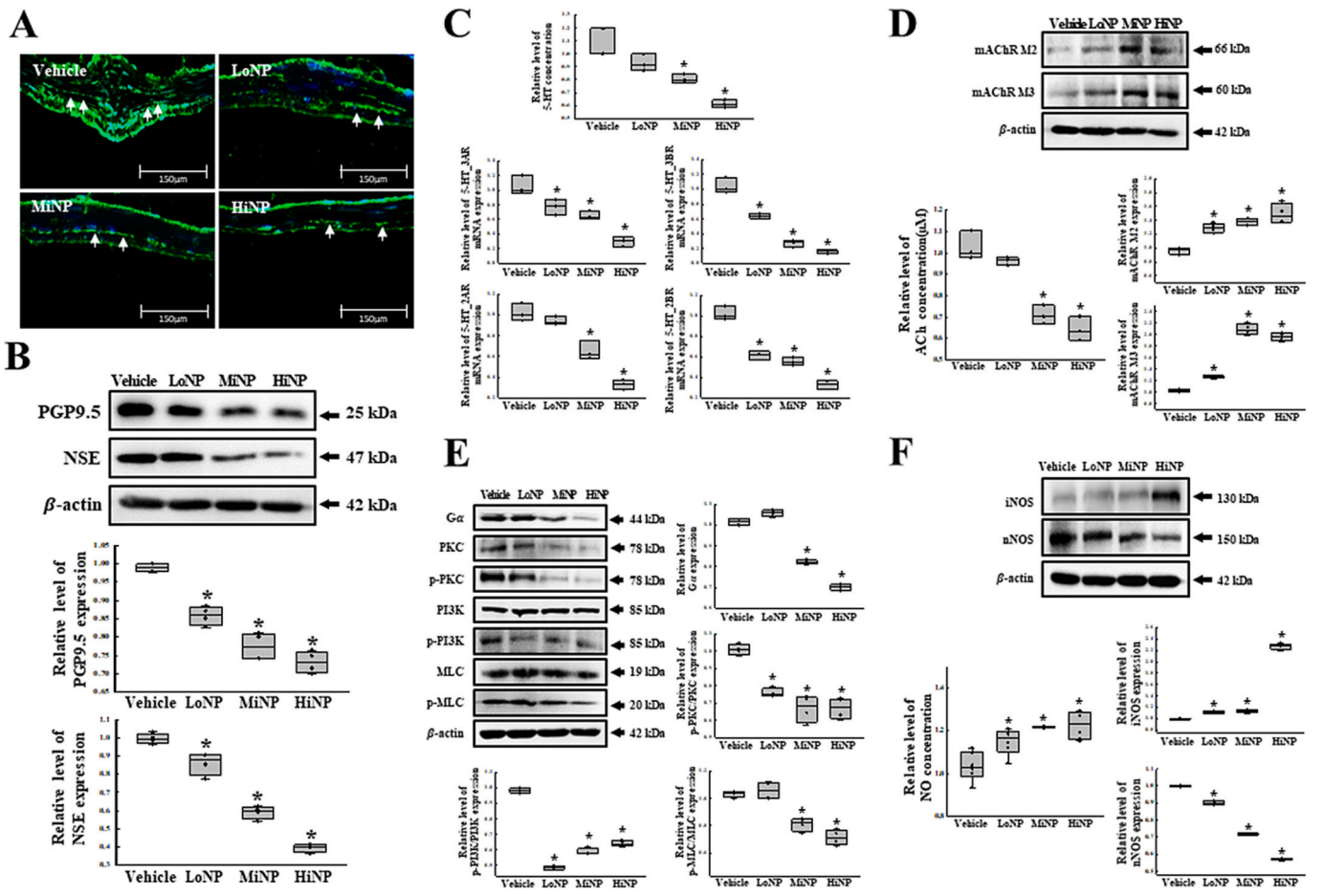

Fig. 5. Regulation of structural and functional parameters for excitatory and inhibitory neuron in the mid-colon of nanoplastics (NPs)-inhaled mice. (A) Tissue distribution of C-kit proteins. (B) Expression levels of protein gene product 9.5 (PGP9.5) and neuron-specific enolase (NSE) proteins. (C) Concentration of 5-hydroxytryptamine (5-HT) and transcription levels of four 5-HT receptors. (D) Concentration of acetylcholine (Ach) and expression levels of muscarinic acetylcholine receptor (mAChR) M2 and M3. (E) Expressions of the key mediators in the mAChR downstream signaling pathway (F) Concentration of nitric oxide (NO), and expression levels of inducible nitric oxide synthase (iNOS) and neuronal nitric oxide synthase (nNOS) proteins. Three to five mice per group were used to prepare the immunofluorescence (IF)-stained sections, total RNA and tissue lysate, and each analysis were conducted in duplicate. The data are reported as the mean ± SD. *, $p < 0.05$ compared to the Vehicle-inhaled group.

for constipation, including decreased stool weight, GI transit, mucin secretion, GI hormone, Cl^- concentration, and the disruption of the histological structure and water balance (Choi et al., 2021). Our findings provide additional direct evidences supporting previous studies that oral administration of NPs can be caused chronic constipation of mice although the method of administration is different. These evidences from our study were primarily demonstrated by analyzing the various phenotypes related with constipation in NPs-inhaled ICR mice. Also, our conclusions on the defecation delay effects of inhaled NPs were verified by the results from intravenous injection of NPs. Therefore, our study using inhalation and intravenous injection strategies of NPs will provide important information on the induction mechanism for constipation induced by NPs in colon.

4.3. Change in the mucin secretion and colonic fluid transport system of mid-colon

The mucin produced from goblet cells plays a key role in various colon functions, including lubrication for food passage, protection of the host epithelium from pathogens and environmental hazards, and participation of cell signaling pathways (Lamont, 1992; Kim and Khan, 2013). In addition, the colonic fluid transport system containing water and electrolytes across the colon mucosa is considered an important step in maintaining water and electrolyte homeostasis of the body (Balcı et al., 2013; Zhao et al., 2021). In particular, the above regulatory factors are significantly disrupted during constipation, including spontaneous or chemical-induced type (Shimotoyodome et al., 2000; Castro-Combs et al., 2014). The above regulatory factors have been considered key targets in the study for the role of MPs as a cause of constipation, but little research has been conducted. The levels of mucin secretion were remarkably decreased in mice after the oral administration of PS-NPs for two weeks or PE-MPs for 30 days (Choi et al., 2021; Sun et al., 2021). Similar decreasing patterns were detected in the transcription levels of AQPs and Cl^- channel and the Cl^- concentration (Choi et al., 2021). In this study, the amount of mucin secreted and transcriptional levels of some ion channels were measured to investigate the defecation delay induced by inhaled NPs in colon of ICR mice. The significant decrease of them detected after NPs inhalation compared to those of Vehicle-inhaled group. These results on the transcription levels of regulators for water and ion were similar to previous studies although more factors were analyzed in our study (Choi et al., 2021). These results provide additional evidence suggesting that the action of inhaled NPs in the mid-colon is closely related to the abnormalities of mucin secretion and colonic fluid transport system function.

4.4. Change in the structure and function of enteric nervous system

The ENS plays a key role in the physiological function of the colon,

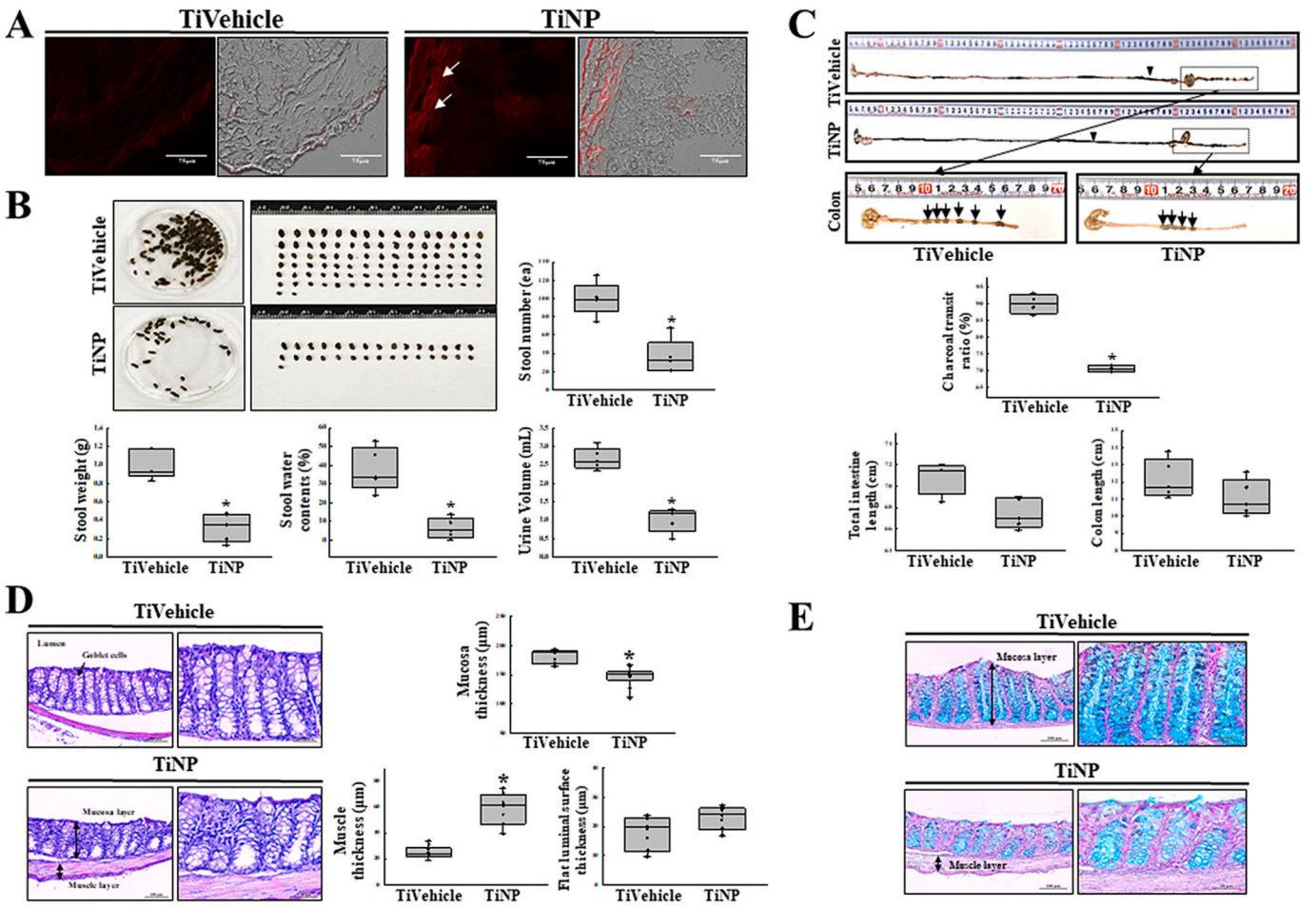

Fig. 6. Determination of the constipation phenotypes in mice intravenously injected with nanoplastics (NPs). (A) Detection of intravenous injected NPs in the colon section. (B) Stools parameters. (C) Gastrointestinal (GI) motility and colon length. (D) Histopathological structure of mid-colon. (E) Mucin secretion of mid-colon. Three to five mice per group were used to prepare the frozen colon sections, total GI tract and H&E-stained sections, and phenotype analyses were assayed in duplicate for each sample. The data are reported as the mean ± SD. *, $p < 0.05$ compared to the Vehicle-injected group.

including GI movements, gastric acid secretion, local blood flow, gut hormones secretion, and immune responses (Rao and Gershon, 2016). Despite the importance of ENS, most research on the effects of NPs focused on the central nervous system (CNS), not ENS. The neuronal arborization and dendritic spine density were disturbed in the prefrontal cortex of Swiss albino mice after oral exposure to PS-NPs (500 nm) for 28 days (Suman et al., 2024). KM mice exposed to PS-MPs (5.0–5.9 μm) showed brain damage, including neuronal loss and disorganization in the hippocampus, decreased ACh levels, and impairments in learning and memory (Wang et al., 2022). Nasal inhalation of 80 nm PS-NPs (PS-COOH and PS-NH_2) was deposited in the brain and inhibited the acetylcholine esterase (AChE) activities (Liu et al., 2022). In addition, the impairment of social behavior in mouse offspring was observed after maternal exposure of PS-MPs (So et al., 2023). Furthermore, the significant neurotoxicity of MPs was detected in various neuronal cells and the brains of mice (Jung et al., 2020; Paing et al., 2024). The only research on the effects of NPs on ENS was reported in the mid-colon of mice that were orally administered PS-MPs for two weeks. Dysregulation of mAChR expression and its downstream signaling pathway was detected in the mid-colons of these mouse (Choi et al., 2021). Our study is the second study to present findings on the potential impact of NPs on the structure and function of ENS in ICR mice although they were not administered directly to the colon. Overall, our results analyzed ICR mice that inhaled NPs were very similar to those of previous study that investigated the effects by orally administered MPs (Choi et al., 2021). Also, the findings of present study show a similar trend to previous studies based on the ability of MPs destroying the structure of CNS and inhibiting its function (Wang et al., 2022; Suman et al., 2024). Furthermore, this study presents the first evidence showing that inhaled NPs can affect the neuronal structure and the regulatory function of excitatory and inhibitory neurons in the ENS of the mid-colon, but more research on the action mechanism is needed.

4.5. *Relationship between intravenous injection of nanoplastic and constipation*

NPs can be distributed and accumulated in various human body organs and tissues through blood vessels after ingestion, inhalation, or skin penetration from the environment (Rajendran and Chandrasekaran, 2023; Li et al., 2024). During these processes, NPs can pass through barrier cells, such as bronchial epithelial cells and endothelial cells, enter the blood circulatory system, and transport other organs, including the liver, intestine, brain, reproductive organ, and bone (Wright and Kelly, 2017). In the blood circulation system, NPs can interact with various blood cells and protein components as well as vascular endothelium, and lead to cytotoxicity, oxidative stress, immunomodulation, and inflammatory response (Ballesteros et al., 2020; Domenech et al., 2023; Rubio et al., 2020). The NPs circulated through the blood vessel can causes various damages, including the impairment of organ function, activation of cells, toxicity, and serious structural injuries in the brain, reproductive organs, liver, and kidney (Shan et al., 2022; Wright and Kelly, 2017; Zha et al., 2024). Nevertheless, intravenous route is

rarely applied as an injection method of NPs, even though the absorption efficacy into blood vessel is higher than other injection routes (Sun et al., 2022). The tail vein injection of PS-NPs for two days inhibits steroidogenic acute regulatory protein (StAR) expression in testicular tissue and stimulates the C-terminus of the Hsc70-interacting protein (CHIP)-mediated degradation of tight junction proteins in Sertoli cells (Sui et al., 2023; Hu et al., 2022). In our study, intravenous injection of NPs was performed to verify the potential of the colon as a secondary target of inhaled NPs. Significant changes in the constipation phenotypes, including the stool parameters, GI transit, histological structure, and mucin secretion were detected in ICR mice intravenously injected with NPs. These results will be provided novel evidence of great value because colon tissue has been never considered as the final targets in the process of NPs transportation through the blood vessel in few previous studies (Shan et al., 2022). In addition, the intravenous injection has been excluded from the main routes of NPs or MPs uptake until now. However, this route in NPs studies has received a lot of attention because some medical devices such as intravenous infusion tubes, syringes and blood needles has been pointed out as the potential sources of human exposure against NPs or MPs (Chen et al., 2025).

4.6. Comparative analysis between oral administration, inhalation, and intravenous injections methods

Finally, the phenotypes for constipation were compared among ICR mice treated with NPs via three different administration routes: oral, inhalation, and intravenous injection (Choi et al., 2021). Despite differences in the specific parameters analyzed, constipation-associated indicators showed similar patterns across three treatment groups, as summarized in Table 1. Nevertheless, the rate of change in each parameter differed between each group. The alteration rate of stool weight, number, water content, and charcoal transit ratio was significantly higher in the intravenous injection group than in the oral administration and inhalation groups (Choi et al., 2021). The decreases in intestine length and gastrin concentration were greater in the inhalation group than in the oral administration and intravenous injection groups, while the highest reductions in water consumption, CCK concentration, and AQP expression were detected in the oral administration group (Choi et al., 2021). Other parameters, including histological structure, mucin secretion, and neuron function, showed similar patterns or no measurement results, making comparisons impossible. The primary cause of this difference on three administration routes for NPs treatment may be the principle of pharmacokinetics, which describes how the body absorbs, distributes, metabolizes, and excretes a substance (van Hoogdalem et al., 1991). Therefore, the above comparison suggests that the inhalation route of NPs can be considered a strong cause of constipation, even though the inducing effect of intravenous injection is somewhat high. Furthermore, the inhalation and intravenous injection of NPs results provide important comparative evidence for the constipation-inducing effects based on NPs exposure routes.

Table 1
Comparison of constipation phenotypes in mice treated with NPs via three different administration routes.

Parameters	Exposure method for NPs		
	Oral administration [16]	Inhalation	Intravenous injection
NPs accumulation in intestine (μg/g)	4.00–29.13	8.77–37.47	High
Decrease level of water consumption (mL/day)	2.71–3.53	1.05–1.13	NA
Decrease level of stool number (ea)	0.14–0.23	0.46–0.69	0.64
Decrease level of stool weight (g)	0.47–0.37	0.60–0.50	0.48
Decrease rate of stool water content (%)	0.42–0.25	0.38–0.19	0.71
Decrease rate of charcoal transit ratio (%)	7.11–13.03	10.01–11.99	16.00
Decrease level of intestine length (mm)	2.00–4.00	8.00–9.50	1.21
Histological structure	Decrease in mucosa, muscle, flat luminal surface, crypt layer thickness	Decrease in mucosa, muscle, flat luminal surface, crypt layer thickness	Increase in muscle, flat luminal surface thickness
Decrease rate of GI hormone (%)	CCK: 29.77–47.97 Gastrin: 9.88–18.98	CCK: 12.93–30.18 Gastrin: 32.18–46.11	NA
Mucin secretion	Decrease	Decrease	Decrease
Decrease rate of water transporters (%)	AQP3: 49.35–83.77 AQP8: 36.97–66.13	AQP3: 21.92–62.08 AQP8: 27.84–70.39	NA
Expression level of ion channels	Decrease	Increase of five, decrease in CIC-2	NA
Number of neurons	NA	Decrease	NA
Function of excitatory neurons	Decrease of mAChR	Disruption	NA
Function of inhibitory neurons	NA	Disruption	NA

Each level was represented the rate or level compared to the Vehicle group. Abbreviations: GI, Gastrointestinal; CCK, Cholecystokinin; AQP, Aquaporin; mAChR, muscarinic acetylcholine receptors; NA, Not applicable.

5. Conclusions

This study examined whether NPs inhalation for two weeks could cause chronic constipation. Constipation-related phenotypes were newly identified in ICR mice that inhaled 500 nm PS-NPs for two weeks, including changes in basic physiological parameters, mucin secretion ability, colonic fluid transport, and ENS function. In addition, similar phenotypes of constipation were detected in ICR mice after the intravenous injection of NPs for two days. These data provide novel evidence that the inhalation and intravenous injection of NPs may be closely related to the induction of constipation and can be considered one of the novel causes of chronic constipation (Fig. 7). Nevertheless, this study had some limitations in evaluating the effects of NPs exposure via inhalation and intravenous injection using particles of varying sizes and materials, and it did not provide sufficient evidence to support translation to human health contexts.

Supplementary data to this article can be found online at https://doi.org/10.1016/j.scitotenv.2025.180789.

CRediT authorship contribution statement

Su Jeong Lim: Validation, Investigation, Formal analysis, Data curation. **Yun Ju Choi:** Validation, Investigation, Formal analysis, Data curation. **Ji Eun Kim:** Investigation, Formal analysis. **Hee Jin Song:** Investigation, Formal analysis. **Ayun Seol:** Investigation, Formal analysis. **Su Ha Wang:** Visualization, Data curation. **Ji Eun Sung:** Investigation, Formal analysis. **Ye Eun Ryu:** Formal analysis. **Ye Ryeong Kim:** Formal analysis. **Woo Bin Yun:** Data curation, Writing – review & editing. **Dae Youn Hwang:** Supervision, Project administration, Methodology, Funding acquisition, Conceptualization, Writing – original draft. **Sungbaek Seo:** Writing – review & editing. **Miran Jang:** Writing –

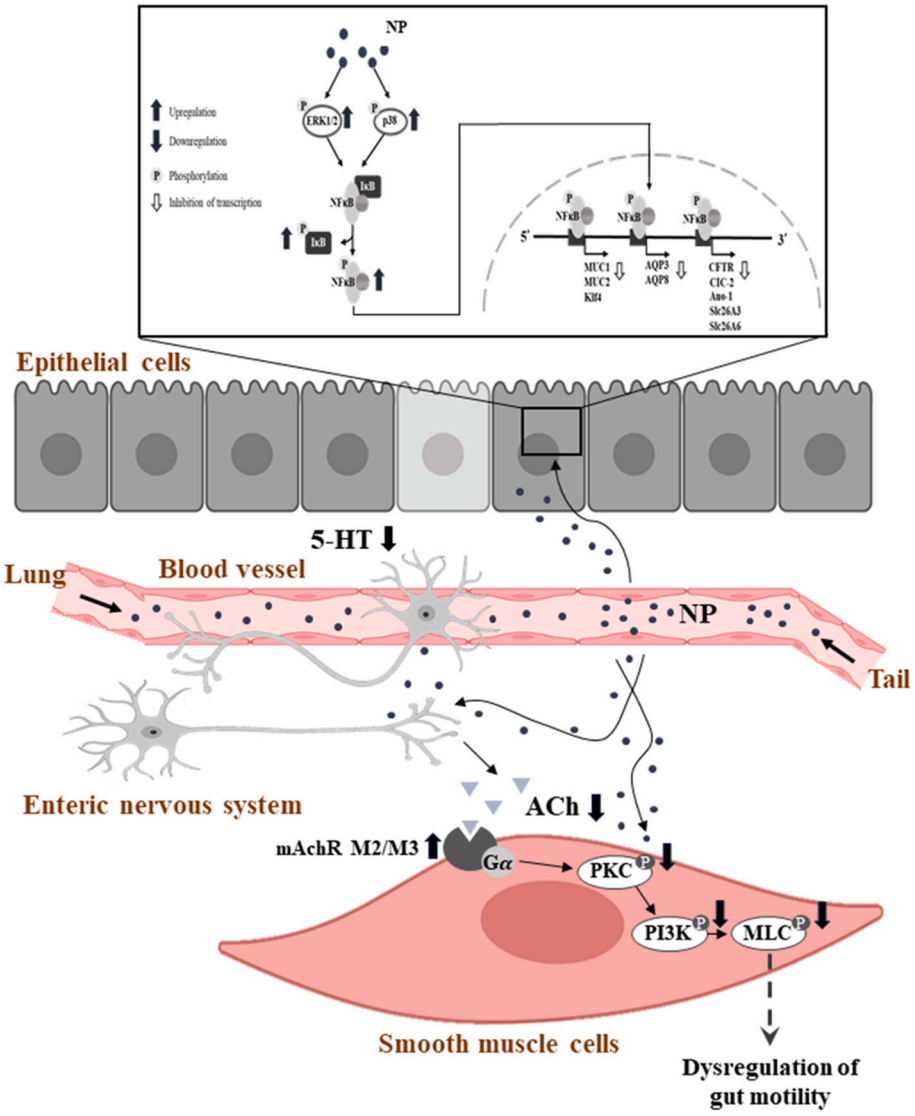

Fig. 7. Suggested action mechanism for constipation in nanoplastics (NPs)-inhaled ICR mice. In this scheme, the inhaled and intravenously injected NPs are translocated to colon of ICR mice through blood vessel. They are thought to be affected by the gut motility through the regulation of muscarinic acetylcholine receptors (mAChRs) downstream signaling pathway in smooth muscle cells, while the expressions of mucin, aquaporin (AQP) and chloride ion channel gene were inhibited by the regulation of nuclear factor kappa B (NF-κB) signaling pathway in the epithelial cells.

review & editing.

Informed consent statement

Not applicable.

Funding

This work was supported by the BK21 FOUR project through the National Research Foundation of Korea (NRF) funded by the Ministry of Education, Korea (F24YY8109033). Also, this research was supported by the Basic Science Research Program through the National Research Foundation of Korea (NRF) funded by the Ministry of Education (RS-2024-00466199).

Declaration of competing interest

The authors declare the following financial interests/personal relationships which may be considered as potential competing interests:

Dae Youn Hwang reports financial support was provided by National Research Foundation of Korea. Su Jeong Lim reports financial support was provided by National Research Foundation of Korea. If there are other authors, they declare that they have no known competing financial interests or personal relationships that could have appeared to influence the work reported in this paper.

Acknowledgments

The authors thank Jin Hyang Hwang, the animal technician, for managing animal care and use at the Laboratory Animal Resources Center in Pusan National University.

Ethics committee approval statement

The study was conducted in accordance with the Declaration of Helsinki and approved by the Pusan National University-Institutional Animal Care and Use Committee (PNU-IACUC) based on the ethical procedures for scientific care (Approval number PNU-2025-0429).

Data availability

Data will be made available on request.

References

Atis, S., Tutluoglu, B., Levent, E., Ozturk, C., Tunaci, A., Sahin, K., Saral, A., Oktay, I., Kanik, A., Nemery, B., 2005. The respiratory effects of occupational polypropylene flock exposure. Eur. Respir. J. 25 (1), 110–117. https://doi.org/10.1183/09031936.04.00138403.

Balcı, A.K., Koksal, O., Kose, A., Armagan, E., Ozdemir, F., Inal, T., Oner, N., 2013. General characteristics of patients with electrolyte imbalance admitted to emergency department. World J Emerg Med 4 (2), 113–116. https://doi.org/10.5847/wjem.j.issn.1920-8642.2013.02.005.

Ballesteros, S., Domenech, J., Barguilla, I., Cortés, C., Marcos, R., Hernández, A., 2020. Genotoxic and immunomodulatory effects in human white blood cells after *ex vivo* exposure to polystyrene nanoplastics. Environ. Sci. Nano 7 (11), 3431–3446. https://doi.org/10.1039/d0en00748j.

Castro-Combs, J., Garcia, C.J., Majewski, M., Wallner, G., Sarosiek, J., 2014. Impaired viscosity of gastric secretion and its mucin content as potential contributing factors to the development of chronic constipation. Dig. Dis. Sci. 59 (11), 2730–2734. https://doi.org/10.1007/s10620-014-3227-y.

Chen, C., Du, S., Liu, Z., Li, W., Tao, F., Qie, X., 2025. Systematic characterisation of microplastics released from disposable medical devices using laser direct infrared spectroscopy. Anal. Chim. Acta 1355, 343982. https://doi.org/10.1016/j.aca.2025.343982.

Choi, Y.J., Park, J.W., Kim, J.E., Lee, S.J., Gong, J.E., Jung, Y.S., Seo, S., Hwang, D.Y., 2021. Novel characterization of constipation phenotypes in ICR mice orally administrated with polystyrene microplastics. Int. J. Mol. Sci. 22 (11), 5845. https://doi.org/10.3390/ijms22115845.

Danso, I.K., Woo, J.H., Lee, K., 2022. Pulmonary toxicity of polystyrene, polypropylene, and polyvinyl chloride microplastics in mice. Molecules 27 (22), 7926. https://doi.org/10.3390/molecules27227926.

Domenech, J., Annangi, B., Marcos, R., Hernández, A., Catalán, J., 2023. Insights into the potential carcinogenicity of micro-and nano-plastics. Mut. Res. Rev. Mut. Res. 791, 108453. https://doi.org/10.1016/j.mrrev.2023.108453.

Ge, Y., Yang, S., Zhang, T., Gong, S., Wan, X., Zhu, Y., Fang, Y., Hu, C., Yang, F., Yin, L., Pu, Y., Chen, Z., Lian, G., 2024. Ferroptosis participated in inhaled polystyrene nanoplastics-induced liver injury and fibrosis. Sci. Total Environ. 916, 170342. https://doi.org/10.1016/j.scitotenv.2024.170342.

Hu, R., Yao, C., Li, Y., Qu, J., Yu, S., Han, Y., Chen, G., Tang, J., Wei, H., 2022. Polystyrene nanoplastics promote CHIP-mediated degradation of tight junction proteins by activating IRE1α/XBP1s pathway in mouse Sertoli cells. Ecotoxicol. Environ. Saf. 248, 114332. https://doi.org/10.1016/j.ecoenv.2022.114332.

Islam, M.S., Rahman, M.M., Larpruenrudee, P., Arsalanloo, A., Beni, H.M., Islam, M.A., Gu, Y.T., Sauret, E., 2023. How microplastics are transported and deposited in realistic upper airways? Phys. Fluids 35 (6). https://doi.org/10.1063/5.0150703.

Jung, B.K., Han, S.W., Park, S.H., Bae, J.S., Choi, J., Ryu, K.Y., 2020. Neurotoxic potential of polystyrene nanoplastics in primary cells originating from mouse brain. Neurotoxicology 81, 189–196. https://doi.org/10.1016/j.neuro.2020.10.008.

Kim, J.J., Khan, W.I., 2013. Goblet cells and mucins: role in innate defense in enteric infections. Pathogens 2 (1), 55–70. https://doi.org/10.3390/pathogens2010055.

Lamont, J.T., 1992. Mucus: the front line of intestinal mucosal defense. Ann. N. Y. Acad. Sci. 664 (1), 190–201. https://doi.org/10.1111/j.1749-6632.1992.tb39760.x.

Li, B., Ding, Y., Cheng, X., Sheng, D., Xu, Z., Rong, Q., Wu, Y., Zhao, H., Ji, X., Zhang, Y., 2020. Polyethylene microplastics affect the distribution of gut microbiota and inflammation development in mice. Chemosphere 244, 125492. https://doi.org/10.1016/j.chemosphere.2019.125492.

Li, X., Zhang, T., Lv, W., Wang, H., Chen, H., Xu, Q., Cai, H., Dai, J., 2022a. Intratracheal administration of polystyrene microplastics induces pulmonary fibrosis by activating oxidative stress and Wnt/β-catenin signaling pathway in mice. Ecotoxicol. Environ. Saf. 232, 113238. https://doi.org/10.1016/j.ecoenv.2022.113238.

Li, Y., Shi, T., Li, X., Sun, H., Xia, X., Ji, X., Zhang, J., Liu, M., Lin, Y., Zhang, R., Zheng, Y., Tang, J., 2022b. Inhaled tire-wear microplastic particles induced pulmonary fibrotic injury via epithelial cytoskeleton rearrangement. Environ. Int. 164, 107257. https://doi.org/10.1016/j.envint.2022.107257.

Li, Y., Chen, L., Zhou, N., Chen, Y., Ling, Z., Xiang, P., 2024. Microplastics in the human body: a comprehensive review of exposure, distribution, migration mechanisms, and toxicity. Sci. Total Environ., 174215 https://doi.org/10.1016/j.scitotenv.2024.174215.

Liu, X., Zhao, Y., Dou, J., Hou, Q., Cheng, J., Jiang, X., 2022. Bioeffects of inhaled Nanoplastics on neurons and alteration of animal behaviors through deposition in the brain. Nano Lett. 22 (3), 1091–1099. https://doi.org/10.1021/acs.

Lu, L., Wan, Z., Luo, T., Fu, Z., Jin, Y., 2018. Polystyrene microplastics induce gut microbiota dysbiosis and hepatic lipid metabolism disorder in mice. Sci. Total Environ. 631, 449–458. https://doi.org/10.1016/j.scitotenv.2018.03.051.

Luo, T., Wang, C., Pan, Z., Jin, C., Fu, Z., Jin, Y., 2019. Maternal polystyrene microplastic exposure during gestation and lactation altered metabolic homeostasis in the dams and their F1 and F2 offspring. Environ. Sci. Technol. 53 (18), 10978–10992. https://doi.org/10.1021/acs.est.9b03191.

Olatunji, G.D., Kokori, E., Ogieuhi, I.J., Chidinma, U.I., Omoworare, O.T., Olatunji, D., Oluwatomiwa, A.V., Oyewale, O.B., Dorcas, O.O., Zuhair, V., Shu, B.I., Stanley, A.C., Aderinto, N., 2024. Nanoplastics as emerging cardiovascular hazards: a narrative review of current evidence. Egypt. J. Intern. Med. 36, 62. https://doi.org/10.1186/s43162-024-00329-1.

Paing, Y.M.M., Eom, Y., Song, G.B., Kim, B., Choi, M.G., Hong, S., Lee, S.H., 2024. Neurotoxic effects of polystyrene nanoplastics on memory and microglial activation: insights from *in vivo* and *in vitro* studies. Sci. Total Environ. 924, 171681. https://doi.org/10.1016/j.scitotenv.2024.171681.

Pauly, J.L., Stegmeier, S.J., Allaart, H.A., Cheney, R.T., Zhang, P.J., Mayer, A.G., Streck, R.J., 1998. Inhaled cellulosic and plastic fibers found in human lung tissue. Cancer Epidemiol. Biomarkers Prev. 7 (5), 419–428.

Rajendran, D., Chandrasekaran, N., 2023. Journey of micronanoplastics with blood components. RSC Adv. 13 (45), 31435–31459. https://doi.org/10.1039/d3ra05620a.

Rao, M., Gershon, M.D., 2016. The bowel and beyond: the enteric nervous system in neurological disorders. Nat. Rev. Gastroenterol. Hepatol. 13 (9), 517–528. https://doi.org/10.1038/nrgastro.2016.107.

Rubio, L., Barguilla, I., Domenech, J., Marcos, R., Hernández, A., 2020. Biological effects, including oxidative stress and genotoxic damage, of polystyrene nanoparticles in different human hematopoietic cell lines. J. Hazard. Mater. 398, 122900. https://doi.org/10.1016/j.jhazmat.2020.122900.

Saha, S.C., Saha, G., 2024. Effect of microplastics deposition on human lung airways: a review with computational benefits and challenges. Heliyon. https://doi.org/10.1016/j.heliyon.2024.e24355.

Shan, S., Zhang, Y., Zhao, H., Zeng, T., Zhao, X., 2022. Polystyrene nanoplastics penetrate across the blood-brain barrier and induce activation of microglia in the brain of mice. Chemosphere 298, 134261. https://doi.org/10.1016/j.chemosphere.2022.134261.

Shaoyong, W., Jin, H., Jiang, X., Xu, B., Liu, Y., Wang, Y., Jin, M., 2023. Benzo [a] pyrene-loaded aged polystyrene microplastics promote colonic barrier injury via oxidative stress-mediated notch signalling. J. Hazard. Mater. 457, 131820. https://doi.org/10.1016/j.jhazmat.2023.131820.

Shimotoyodome, A., Meguro, S., Hase, T., Tokimitsu, I., Sakata, T., 2000. Decreased colonic mucus in rats with loperamide-induced constipation. Comp. Biochem. Physiol. A Mol. Integr. Physiol. 126 (2), 203–212. https://doi.org/10.1016/s1095-6433(00)00194-x.

So, Y.H., Shin, H.S., Lee, S.H., Moon, H.J., Jang, H.J., Lee, E.H., Jung, E.M., 2023. Maternal exposure to polystyrene microplastics impairs social behavior in mouse offspring with a potential neurotoxicity. Neurotoxicology 99, 206–216. https://doi.org/10.1016/j.neuro.2023.10.013.

Sui, A., Yao, C., Chen, Y., Li, Y., Yu, S., Qu, J., Wei, H., Tang, J., Chen, G., 2023. Polystyrene nanoplastics inhibit StAR expression by activating HIF-1α via ERK1/2 MAPK and AKT pathways in TM3 Leydig cells and testicular tissues of mice. Food Chem. Toxicol. 173, 113634. https://doi.org/10.1016/j.fct.2023.113634.

Suman, A., Mahapatra, A., Gupta, P., Ray, S.S., Singh, R.K., 2024. Polystyrene microplastics induced disturbances in neuronal arborization and dendritic spine density in mice prefrontal cortex. Chemosphere 351, 141165. https://doi.org/10.1016/j.chemosphere.2024.141165.

Sun, A., Wang, W.X., 2023. Human exposure to microplastics and its associated health risks. Environ. Health 1 (3), 139–149. https://doi.org/10.1021/envhealth.3c00053.

Sun, H., Chen, N., Yang, X., Xia, Y., Wu, D., 2021. Effects induced by polyethylene microplastics oral exposure on colon mucin release, inflammation, gut microflora composition and metabolism in mice. Ecotoxicol. Environ. Saf. 220, 112340. https://doi.org/10.1016/j.ecoenv.2021.112340.

Sun, W., Jin, C., Bai, Y., Ma, R., Deng, Y., Gao, Y., Pan, G., Yang, Z., Yan, L., 2022. Blood uptake and urine excretion of nano-and micro-plastics after a single exposure. Sci. Total Environ. 848, 157639. https://doi.org/10.1016/j.scitotenv.2022.157639.

van Hoogdalem, E., de Boer, A.G., Breimer, D.D., 1991. Pharmacokinetics of rectal drug administration, part I. General considerations and clinical applications of centrally acting drugs. Clin. Pharmacokinet. 21 (1), 11–26. https://doi.org/10.2165/00003088-199121010-00002.

Wang, J., Tian, H., Shi, Y., Yang, Y., Yu, F., Cao, H., Gao, L., Liu, M., 2023. The enhancement in toxic potency of oxidized functionalized polyethylene-microplastics in mice gut and Caco-2 cells. Sci. Total Environ. 903, 166057. https://doi.org/10.1016/j.scitotenv.2023.166057.

Wang, S., Han, Q., Wei, Z., Wang, Y., Xie, J., Chen, M., 2022. Polystyrene microplastics affect learning and memory in mice by inducing oxidative stress and decreasing the level of acetylcholine. Food Chem. Toxicol. 162, 112904. https://doi.org/10.1016/j.fct.2022.112904.

Wright, S.L., Kelly, F.J., 2017. Plastic and human health: a micro issue? Environ. Sci. Technol. 51 (12), 6634–6647. https://doi.org/10.1021/acs.est.7b00423.

Wu, Q., Liu, C., Liu, Dan, Wang, Y., Qi, H., Liu, X., Zhang, Y., Chen, H., Zeng, Y., Li, J., 2024. Polystyrene nanoplastics-induced lung apoptosis and ferroptosis via ROS-dependent endoplasmic reticulum stress. Sci. Total Environ. 912, 169260. https://doi.org/10.1016/j.scitotenv.2023.169260.

Wu, Y., Yao, Y., Bai, H., Shimizu, K., Li, R., Zhang, C., 2023. Investigation of pulmonary toxicity evaluation on mice exposed to polystyrene nanoplastics: the potential protective role of the antioxidant N-acetylcysteine. Sci. Total Environ. 855, 158851. https://doi.org/10.1016/j.scitotenv.2022.158851.

Xie, L., Chen, T., Liu, J., Hou, Y., Tan, Q., Zhang, X., Li, Z., Farooq, T.H., Yan, W., Li, Y., 2022. Intestinal flora variation reflects the short-term damage of microplastic to the intestinal tract in mice. Ecotoxicol. Environ. Saf. 246, 114194. https://doi.org/10.1016/j.ecoenv.2022.114194.

Yang, S., Zhang, T., Ge, Y., Cheng, Y., Yin, L., Pu, Y., Chen, Z., Liang, G., 2023. Ferritinophagy mediated by oxidative stress-driven mitochondrial damage is involved in the polystyrene nanoparticles-induced ferroptosis of lung injury. ACS Nano 17 (24), 24988–25004. https://doi.org/10.1021/acsnano.3c07255.s001.

Zha, H., Xia, J., Wang, K., Xu, L., Chang, K., Li, L., 2024. Foodborne and airborne polyethersulfone nanoplastics respectively induce liver and lung injury in mice: comparison with microplastics. Environ. Int. 183, 108350. https://doi.org/10.1016/j.envint.2023.108350.

Zhan, Y., Tang, X., Xu, H., Tang, S., 2020. Maren pills improve constipation via regulating AQP3 and NF-κB signaling pathway in slow transit constipation *in vitro* and *in vivo*. Evid. Based Complement. Alternat. Med. 2020, 9837384. https://doi.org/10.1155/2020/9837384.

Zhang, S., Zhang, H., Li, Y., Sun, Z., Chen, Y., 2024. Recent advances on transport and transformation mechanism of nanoplastics in lung cells. Sci. Total Environ. 952, 175881. https://doi.org/10.1016/j.scitotenv.2024.175881.

Zhang, T., Yang, S., Ge, Y., Wan, X., Zhu, Y., Yang, F., Li, J., Gong, S., Cheng, Y., Hu, C., Chen, Z., Yin, L., Pu, Y., Liang, G., 2023. Multi-dimensional evaluation of cardiotoxicity in mice following respiratory exposure to polystyrene nanoplastics. Part. Fibre Toxicol. 20 (1), 46. https://doi.org/10.1186/s12989-023-00557-3.

Zhao, Q., Chen, Y.Y., Xu, D.Q., Yue, S.J., Fu, R.J., Yang, J., Xing, L.M., Tang, Y.P., 2021. Action mode of gut motility, fluid and electrolyte transport in chronic constipation. Front. Pharmacol. 12, 630249. https://doi.org/10.3389/fphar.2021.630249.